Calculations of the dimensional dependence of the critical state in disk-shaped superconductors

L. W. Conner and A. P. Malozemoff
IBM Research, Yorktown Heights, New York 10598-0218
(Received 6 June 1990; revised manuscript received 24 August 1990)

We present numerical calculations of the field distribution and the moment of disk-shaped superconductors in the critical state, extending earlier work of Daeumling and Larbalestier. In particular, using the Kim model for the dependence of critical current density on field, we show that a conventional model ignoring flux-line curvature predicts a nonlinear dependence of zero-field remanent moment on radius, while accounting for the curvature numerically leads to an almost linear dependence on radius, with a slope reduced from that of the Bean formula. We find an approximate analytical formula for this reduced slope.

I. INTRODUCTION

In this paper we present numerical calculations of the magnetic field distribution and magnetic moment of a disk-shaped superconductor in the critical state.[1,2] This is of special interest in the context of high-temperature superconductivity where most magnetic data have been taken on platelet-shaped crystals or thin films with applied fields perpendicular to the plane. The large demagnetizing effects complicate the interpretation of this configuration, but it is important to understand this case since alignment problems and signal strength problems make the in-plane measurements difficult, and since in any case the materials are so anisotropic.

A conventional approach[3,4] to treat shape effects is to use the demagnetizing factor N defined in terms of an ellipsoidal approximation to the sample shape and to correct the applied field H_a by the demagnetizing field $-NM$, where M is the magnetization. However a number of authors[5,6] have recently pointed out that in the critical state of a superconductor, in which current is uniformly distributed in the bulk, this is wrong not only quantitatively but qualitatively. In particular, Daeumling and Larbalestier[6] performed numerical calculations on a disk of radius R and thickness $D << R$, which showed that for a uniform bulk circumferential current density J_c, the field distribution and hence the vortex lines within the superconductor become severely curved, even though the conventional Bean formula[1] for the remanent magnetization M_{rem} (in mks units with $B=\mu_0 H+\mu_0 M$)

$$M_{\text{rem}}=J_c\frac{R}{3} \tag{1}$$

remains unchanged. However when the current density depends on field, for example, using the Kim form[7]

$$J_c(H)=\alpha/(H+H_0)\ , \tag{2}$$

where α and H_0 are constants, then Daeumling and Larbalestier[6] suggested that the moment would depend on field and radius in a more complicated way. They calculated one example of the field dependence $M_{\text{rem}}(H)$.

Here we focus on the radius dependence of the remanent moment ($H_a=0$). Since Eq. (1) has been so widely used to determine critical current densities of films and crystals of high temperature superconductors, it is clearly important to test its validity by studying the radius dependence experimentally. The results so far in the literature are ambiguous, with reports of both nonlinear[8-12] and linear[4,13-15] behaviors. In particular, the data of Oh *et al.*,[13] evaluated from their hysteresis loops even at $H_a=0$, show good linearity over a wide range of sizes for a patterned Y-Ba-Cu-O film. Yeshurun *et al.*[4] observe linearity only over a more modest range in patterned thin Y-Ba-Cu-O and Bi-Sr-Ca-Cu-O crystals. Since nonlinearity can arise from granularity or weak links, we presume that this more rarely observed linear behavior characterizes the most homogeneous material, though clearly further experimental work is required in this area.

The linear results have been interpreted as support for the Bean model and for bulk (rather than edge) current flow in nongranular crystals and films of the high-temperature superconductors. However, at remanence they actually pose something of a contradiction when interpreted in a conventional model which assumes *straight* vortices lying perpendicular to the disk plane. For this case we will show in Sec. II that $M(R)$ should be *nonlinear* whenever—as is in fact the case[4,13,14]—J_c depends on field. The resolution to this contradiction is to consider *curvature* of the vortices, that is, both radial and axial components of magnetic field and flux in the superconductor. This complex geometry requires numerical electromagnetic calculations extending those of Frankel[5] and Daeumling and Larbalestier;[6] we describe the calculations and results in Sec. III. Finally, in Sec. IV we interpret the results and derive an approximate formula which gives physical insight into this complex behavior and which should be useful for estimating the suppression of the slope dM_{rem}/dR below the Bean value in Eq. (1). Here we consider only an isotropic field-dependence of J_c; the effects of critical current anisotropy are a topic for further work.

II. CONVENTIONAL MODEL

We calculate here the dependence of moment on radius for a conventional critical state model with a field-dependent critical current density of the Kim form, Eq. (2). By "conventional model" we mean here a model in which the vortices are assumed to stand vertical, perpendicular to the plane of the disk. Now Maxwell's equation

$$\nabla \times \mathbf{H} = \mathbf{J} \tag{3}$$

in general has *two* terms dH_z/dr and dH_r/dz with a circumferential current J, but for vertical vortices, $H_r = dH_r/dz = 0$; so Eq. (3) reduces to $dH_z/dr = J$. We emphasize this point because in fact this approximation is grossly wrong for the disk-shaped geometry, as has been pointed out by Daeumling and Larbalestier,[6] and the opposite limit will be discussed in Sec. IV. Nevertheless we proceed here with this approximation since it underlies so much conventional thinking about this problem and since it will provide an interesting contrast to the correct answer.

To perform the calculation we integrate Eq. (3) with the field-dependent J_c of Eq. (2):

$$H_z(r,R) = \sqrt{H_0^2 + 2\alpha(R-r)} - H_0 \ . \tag{4}$$

Next we set B equal to $\mu_0 H$ inside the material, assuming the equilibrium M to be negligibly small. This is equivalent to assuming that H_{c1} is small compared to the other fields in the problem, like H_0 in Eq. (2), or the self-fields. Finally we integrate B over the volume of the disk and divide by volume to get the magnetization of the disk.

To write the result we use a normalization which we will apply throughout the article. We normalize distances to the disk thickness D and fields to the natural field units implied by Eq. (2), namely, $\sqrt{\alpha D}$. It is further convenient to define a second normalization for radius in terms of h_0. We use lower-case letters for normalized quantities. Thus we define

$$r_0 \equiv R/D \ , \tag{5}$$

$$h_0 \equiv H_0/(\alpha D)^{1/2} \ , \tag{6}$$

$$m \equiv \frac{M}{(\alpha D)^{1/2}} \ , \tag{7}$$

$$x \equiv R\alpha/H_0^2 \equiv r_0/h_0^2 \ . \tag{8}$$

With this notation we write the result for the normalized dependence of remanent magnetization m on radius x:

$$m = h_0[2(1+2x)^{5/2} - 15x^2 - 10x - 2]/15x^2 \ . \tag{9}$$

Equation (9), plotted as the solid line in Fig. 1, is clearly nonlinear with radius. This nonlinearity comes from the self-fields $H(r)$ which build up from the edge into the center of the disk, causing $J_c(H)$ to drop. It is obvious that if R is small enough, these self-fields will be small compared to H_0, and so J_c will be essentially constant. In this limit Eq. (9) should, and does, reduce to the usual Bean formula Eq. (1), which is just $m = h_0 x/3$ in the normalized units, and which is shown as a dotted line, extrapolated from the $x \to 0$ limit.

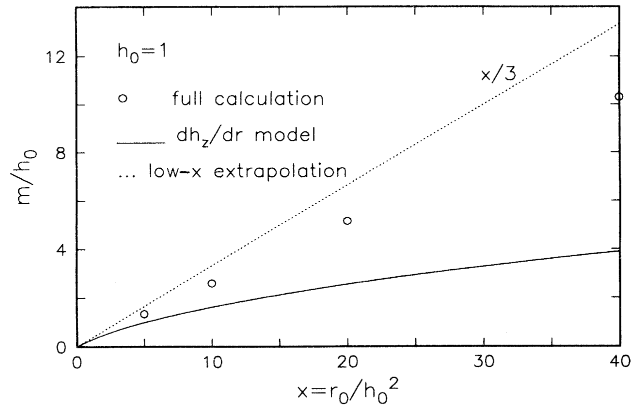

FIG. 1. Normalized magnetization as a function of a normalized radius of a disk with circumferential critical supercurrents. The current is assumed to depend on field according to the Kim form, Eq. (2) [normalized parameters in Eqs. (5)–(8)]. Circles represent full electromagnetic calculations with $h_0 = 1$, the solid line represents Eq. (9), and the dotted line represents Eq. (1) (Bean model). The reduced slope of the circles as compared to the Bean model is described by the "slope reduction factor" of Fig. 4.

Typical experiments[4,13,14] on thin films and crystals of Y-Ba-Cu-O at low temperature should be well into the nonlinear region, as the following estimate shows. At low temperatures, these materials have J_c of order 2×10^{10} A/m^2 for crystals and more for films, and field dependences which can be fit to Eq. (2), giving values of order $\mu_0 H_0 \simeq 0.5$ T and $\mu_0\alpha \simeq 10^{10}$ AT/m^2. The radius beyond which the self-field becomes comparable to H_0 is H_0/J_c or about 25 μm, significantly smaller than the lateral dimension of most samples.

Thus the question becomes, could linearity of remanent moment with radius be observed in these samples at all? The answer comes from treating the full problem, and in particular from recognizing that the fields do not lie just perpendicular to the disk but are curved, generating a dominant gradient in dH_r/dz rather than in dH_z/dr, as we shall see in the next section.

III. NUMERICAL CALCULATIONS

We describe here the calculation of the field and current distributions in a superconducting disk in a remanent critical state with bulk current flow. We assume thickness large compared to the penetration depth and are thus ignoring additional local energies arising from vortex bending or from London surface supercurrents. In cylindrical coordinates, the radial and axial magnetic field components at some point r and z, generated by a ring of radius a, centered at the origin and carrying a current I, are given by[16]

$$H_r(a,r,z)=\frac{I}{2\pi r}\frac{z}{[(a+r)^2+z^2]^{1/2}}\left[-K(k)+\frac{a^2+r^2+z^2}{(a-r)^2+z^2}E(k)\right], \tag{10}$$

$$H_z(a,r,z)+\frac{I}{2\pi}\frac{1}{[(a+r)^2+z^2]^{1/2}}\left[K(k)+\frac{a^2-r^2-z^2}{(a-r)^2+z^2}E(k)\right], \tag{11}$$

where $k^2=4ar[(a+r)^2+z^2]^{-1}$ and where K and E are complete elliptic integrals of the first and second kind. The magnetic field at any point generated by assumed azimuthal (circumferential) current distribution in a disk can be found by integrating these equations over the volume of the disk. Since we assume H_{c1} to be negligible, we take this field within the sample to be the spatially averaged local magnetic induction carried by the vortices.

To integrate Eqs. (10) and (11) we have used a method similar to Romberg's integral method,[17] but instead of using an extended trapezoid rule we have used an extended midpoint rule. There were two reasons for this choice. Unlike other methods used in numerical integration, both the extended trapezoid rule and the extended midpoint rule have an error series that is completely even with step size.[18] This causes the error to fall off rapidly with successive refinements in the evaluation of the integral. But unlike the trapezoid rule, the midpoint rule does not require the integral to be evaluated at the end points of the subinterval. This helped to avoid divergence in the integrals when $a=r$, and z was small. As in the Romberg method, the first refinements to the evaluation of the integral were made by decreasing the step size, reevaluating the integral, and combining the new value with the previous value in a way which decreases the error. Since this is a double integral over r and z, the integral over r had to be evaluated to the desired accuracy for each subinterval of z. Therefore, as the step size in z was decreased to improve the accuracy of the integral over z, the number of integrals over r which had to be evaluated also increased. To reduce the amount of computer time needed to achieve the desired accuracy, the reduction in step size was combined with an extrapolation technique. The evaluation from each reduction in step size was stored. These values were used to construct an interpolating polynomial using Neville's algorithm[18,19] and the evaluation for the integral with zero step size was extrapolated. If the estimated error in this evaluation was not within an acceptable limit the step size was decreased, the integral was reevaluated using the extended midpoint rule, the interpolating polynomial was updated, and a new evaluation for zero step size was extrapolated.

Using this procedure we calculated the values of H_r and H_z at a number of points within the disk. For the case of constant current density, we recovered the results reported by Daeumling and Larbalestier.[6] We then investigated the case of isotropic but field-dependent current density using the Kim form, Eq. (2). Since the field strength depends on the current density, which in turn depends on the field strength, these equations were solved iteratively. Furthermore, since the field strength at any point depends on the current density throughout the entire disk it was necessary to solve for the fields at every point in the disk simultaneously. To do this we started with either a current density chosen from experience or a constant current density. We chose a grid of points within the volume of the disk, and using the initial current density we integrated Eqs. (10) and (11) for each point on the grid. The current density throughout the disk was then calculated from the fields using Eq. (2) and used to calculate the new values of the fields. This procedure was continued until a self-consistent solution was reached for each point, simultaneously. In the course of integrating H_r and H_z it was necessary to determine the values of the current density at points which were not on the grid. Since it was necessary to interpolate in two dimensions, thus potentially adding a significant amount of error, and since the current density often changed rapidly, we used an interpolating polynomial to find the current density at a specific point. Again employing Neville's algorithm we used 3 to 5 points to interpolate the values of the current density at a series of 3 to 5 values of z, for a specific r. We then interpolated between these values to find the current density at the desired point.

Several factors affected convergence. In addition to the usual problems, including divergence, oscillations, and chaotic behavior, that one can encounter when solving an iterative problem, there were the added problems caused by the nature of the equations. H_r and H_z are both dependent on J, which in turn depends on both H_r and H_z. This makes H_r and H_z indirectly dependent on each other. Because of this interdependency any error in either H_r or H_z affected the evaluation of both in the next iteration. At any point in the calculation H_r, for instance, may be converging. However, the error in H_r, even though it is decreasing, may cause the error in H_z to increase. Eventually the error in H_z will affect H_r and cause it to move away from its correct solution. For this reason it was necessary to closely monitor the progress of the calculation to make sure it was actually moving toward a solution. Another serious complication was the propagation of these errors. This comes from the fact that H_r and H_z at any point are calculated by integrating Eqs. (10) and (11) over the volume of the disk. Therefore an error in the field strength at any point will cause an error in the calculation of the fields at every point. Because of this the degree of accuracy to which we held the integration had a strong affect on convergence. Increasing the amount of error allowed in the integration greatly increased the problems of getting the calculation to converge, while decreasing the amount of error allowed greatly increased the time necessary to complete an iteration. We found that a good compromise was to hold the error in the integration to within 10^{-3}. Another factor which affected the convergence was the number of points within the disk at which the fields were calculated. Increasing the number of points obviously increased the amount of time required to complete each iteration, but decreasing the number of points often increased the number of iterations necessary to reach convergence. There are several possible reasons for this, the most obvious being that the current density often changed less rapidly from point to point as these points were moved closer. With a smoother change interpolation between points was more accurate leading to a more accurate integrand from Eqs. (10) and (11), which in turn lead to a more accurate evaluation of H_r and H_z at every point. We were not able to find a specific number of points which optimized efficiency. For each new set of parameters it was necessary to start with a guess and based on experience increase or decrease the number of points according to how the calculation was progressing. We generally used between 2000 and 7000 points. To accelerate convergence we also used several techniques including the weighted averaging of data from previous iterations, the selective averaging of data within an iteration, and the smoothing of data over a carefully chosen number of points.

As a final word on convergence, we briefly point out that there is nothing in the equations which guarantees a unique mathematical solution. All we can demand with our iterative method is a current density which reproduces itself via Eqs. (2), (10), and (11). While we believe there is only one physically correct solution, there may be multiple current densities which satisfy the purely mathematical requirement. To increase the likelihood that we had arrived at a correct solution we repeated the calculation using a different current density or a greater number of points.

An example is shown in Fig. 2(a), where the radial field at the surface and the axial field at the midplane are shown as a function of normalized radial position r for the case $h_0 \equiv H_0/\sqrt{\alpha D}=0.5$, and for two different values of radius $r_0 \equiv R/D=5$ and 15. There remains a small amount of scatter in the curve of H_z for $R/D=15$ even though the solution was stable. We found that the larger values of R/D required the calculation of a greater number of points to get a smooth curve. In the calculation for this curve we used 6480 points. Our experience with the calculations at smaller radii showed that increasing the number of points smoothed out the curve without significant shifts in its position. Since the calculation already involved considerable computer time, we did not increase the number of points any further in the $R/D=15$ case of Fig. 2 because it was not likely to produce significantly new information.

The results are qualitatively similar to those of Daeumling and Larbalestier[6] for the simple case of constant J_c, and also to those of Frankel,[5] who used the Kim form for J_c but showed results only for the axial field at the surface. The most remarkable feature of Fig. 2 is in fact the size of the radial field at the surface. Since by symmetry the radial field is zero at the midplane and changes sign at the bottom surface, the values of H_r in Fig. 2(a) indicate a large gradient dH_r/dz through the

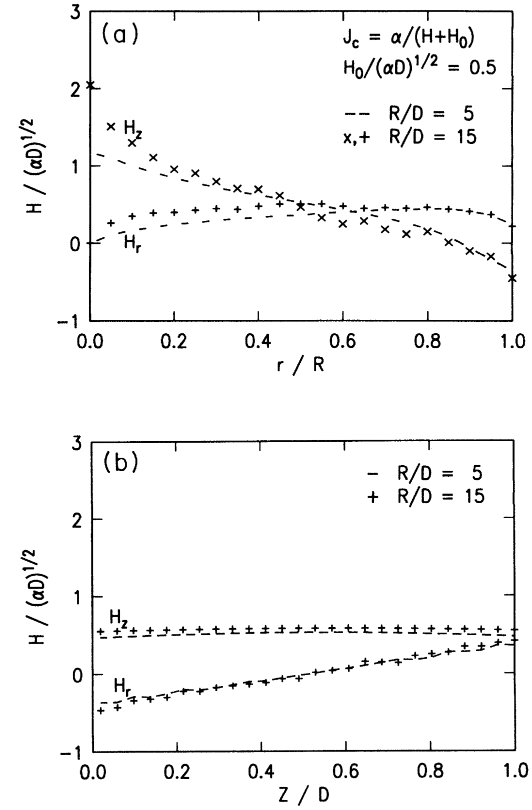

FIG. 2. The radial (H_r) and axial (H_z) fields with a field dependent current density $J=\alpha/(H_0+H)$, for $h_0=0.5$ [normalized units, $h_0=H_0/(\alpha D)^{1/2}$]. The dashed lines show data for a disk with $r_0 \equiv R/D=5$, the plus signs show data for a disk with $r_0=15$. (a) Shows the radial dependence of these fields, from the center of the disk to the edge. H_z was calculated in the center plane of the disk, H_r was calculated at the surface. (b) Shows the axial dependence of the fields from the bottom to the top of the disk, at a position of one-half the maximum radius of the disk.

thickness of the disk, which is only weakly dependent on radius except at the very center and outer edge, and which does not depend strongly on the outside radius R. This is confirmed in Fig. 2(b), which shows both the radial and axial fields through the thickness of the disk, at a radial position of one-half the full radius of the disk.

Figure 2(b) also shows that the axial field is roughly constant through the thickness of the film, while Fig. 2(a) exhibits a gradient of H_z along the radius. The strength of this gradient can be estimated from the tangent to the $H_z(r)$ curve at the middle of the figure. It is reduced from the vertical gradient by a ratio of order D/R, just as in the case[6] of constant J_c.

Further insight comes from the contour plot of the critical current density distribution through a cross section of the disk, shown in Fig. 3. This calculation is for the case of the Kim form for $J_c(H)$ with $h_0=0.5$ and $R/D=5$. The J_c contours run in steps of 0.05 from 0.6 near the center of the disk ($r=0$ in the figure) up to 2 at a peak in the midplane near the outer edge (the critical current density is normalized by $\sqrt{\alpha/D}$). The reason for

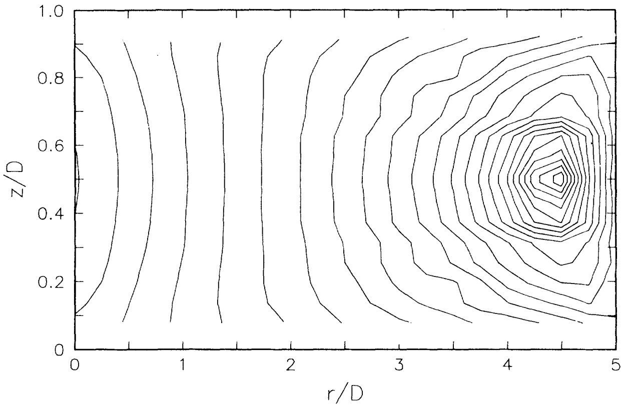

FIG. 3. Contour plot of current distribution in a cross section of one-half of a disk, for the case of a Kim field-dependent critical current density with $h_0=0.5$. In this plot $r=0$ represents the center of the disk, $r/D=5$ the outside edge. The contours, in units of $\sqrt{\alpha/D}$, run in steps of 0.05 from 0.6 at the center to almost 2 at the peak near the outside edge. The peak in current density is related to the zero crossing in both H_z and H_r at the midplane near the outer edge, as shown in Fig. 2.

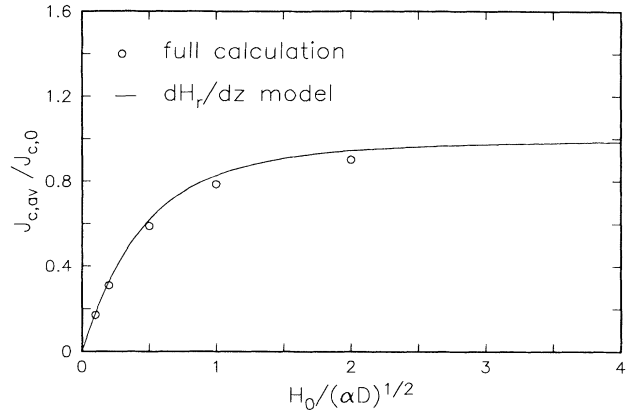

FIG. 4. A magnetization-vs-radius slope reduction factor (circles from calculated slopes as in Fig. 1) as a function of the normalized Kim parameter $h_0=H_0/(\alpha D)^{1/2}$. The solid line represents Eq. (13), the normalized current density calculated from Maxwell's equation using only the dH_r/dz term.

the peak is that at this point, both H_z and H_r are zero, as shown in Fig. 2, and so J_c in Eq. (2) has a maximum. Some irregularity in the contours comes in part from the coarseness of the grid used in making this plot.

The similarities of the above results with previous calculations[5,6] dictate similar conclusions: the dominant gradient which sustains the critical current density according to Maxwell's equation (3) is not dH_z/dr, as conventionally assumed, but is dH_r/dz, and it dominates in proportion to the ration R/D, which can be very large in a film or a crystal platelet. This means that the vortex lines are strongly curved and the critical state gradient is predominantly through the thickness of the disk. The main difference from the case of constant J_c is in the absolute value of the gradient. Rather than dH_r/dz equaling J_c, we find it to be reduced in our case well below the low-field limit $J_c \rightarrow \alpha/H_0$, evidently because of self-fields which exceed H_0 and therefore lower J_c in Eq. 2.

Finally, the magnetization was calculated by integrating the magnetic moment $\pi a^2 I$ of a current loop over the entire volume of the disk, and dividing by the volume. For a particular a and z we calculated I from an interpolated value of H, after the final iteration. In these calculations we explored a range of values of normalized radius $r_0 \equiv R/D=2$ to 200, and normalized field $h_0 \equiv H_0/\sqrt{\alpha D}$ from 0.1 to 2.

Results are shown in Fig. 1 for the case $h_0=1$ and are compared to the predictions of the "conventional" or "dH_z/dr" model of Sec. II. The calculated magnetizations, represented by the circles, lie substantially above the earlier model and form a rather straight line as a function of radius. Clearly the line cannot extrapolate precisely through the origin, because in the limit of small radius, where the limit of a thin cylinder is approached, the conventional model becomes valid and the slope approaches Eq. (1), which in the normalized units of the figure is just $x/3$. Nevertheless this is only a small correction. The straight-line slopes determined from two nonzero data points from the numerical calculations for different values of h_0 are summarized as circles in Fig. 4.

IV. DISCUSSION

The discovery that the calculated magnetization depends approximately linearly on radius is the main result of this paper. This is to be contrasted to the conventional model with a field-dependent current density, where the magnetization depends on radius in a much more nonlinear way. The underlying reason for the new result is that the critical state gradient develops predominantly through the thickness rather than along the radius of the disk. These observations may help explain those experimental results[4,13–15] where radius linearity is found along with a strongly field-dependent J_c.

There remains the question of what determines the linear slope, which lies below that predicted in the simple Bean formula of Eq. (1) [we are assuming here that $J_{c,0}$ is taken to be the low-field limit of Eq. (2), namely, α/H_0]. It would be desirable to have an analytical formula to permit extracting the critical current density from measurements of the remanent moment without an elaborate numerical calculation. The similarity of Fig. 2 to the earlier calculation of Daeumling and Larbalestier[6] suggests a simple interpretation of our results and an approach to the problem of deriving an analytical formula. The key notion is that since the critical state gradient is oriented predominantly through the thickness of the disk, and since the thickness is small, one can *average* the current through the thickness of the disk, and that this averaged current, uniform along most of the radius, is sufficient to determine the main features of the field distribution. Figure 3 shows that except for the current density peak near the outer edge, the distribution is sufficiently uniform to make this a reasonable starting approximation.

To perform this calculation we ignore the dH_z/dr term of Maxwell's equation (3) (this is the *opposite* limit to that in Sec. II), which should be accurate to order D/R according to our calculations. Thus we can integrate for the thickness dependence of the radial field H_r, obtaining an equation exactly like Eq. (4), with $(R-r)$ replaced by z measured from the surface. Inserting this result into the Kim form Eq. (2) for the field-dependent current density and integrating over thickness, we obtain the averaged current density

$$J_{c,\mathrm{av}}=2\sqrt{\alpha/D}\,(\sqrt{h_0^2+1}-h_0)\ , \tag{12}$$

with $h_0=H_0/\sqrt{\alpha D}$ as before. Since this averaged current density is roughly uniform with radius, the magnetization becomes just Eq. (1), but with J_c replaced by $J_{c,\mathrm{av}}$. With $J_{c,0}\equiv\alpha/H_0$ we can derive the slope reduction factor

$$J_{c,\mathrm{av}}/J_{c,0}=2h_0(\sqrt{h_0^2+1}-h_0)\ . \tag{13}$$

Referring to Fig. 1, this slope reduction factor should represent the ratio of the true slope (e.g., the calculated circles in the figure) to the Bean model slope (the dashed line).

Equation (13) is plotted as a function of h_0 in Fig. 4, where it is compared to the calculated slopes. The agreement is good, which confirms the validity of the underlying physical concepts. Equation (13) shows a saturation above a characteristic value $h_0\simeq 1$, which corresponds to the condition $H_0\simeq J_{c,0}D$. The interpretation is that as soon as H_0 is larger than the self-fields $J_{c,0}D$ generated by Maxwell's equation and the critical state through the thickness of the disk, the current density of Eq. (3) becomes field independent, and so the reduction factor of Eq. (13) approaches 1. The formula is valid only in the regime $x>1$ in Fig. 1, where x is the normalized radius of Eq. (8). This is equivalent to the condition $J_{c,0}R>H_0$.

In summary, Eq. (13) should give a simple correction for future determinations of critical current density from the Bean model and the zero-field remanent moment. Further calculations are clearly of interest to study the applied field dependence of the remanent moment and also the anisotropy in the critical currents, both of which have been ignored here. These are planned to be addressed in future work.

ACKNOWLEDGMENTS

The authors thank M. Daeumling, R. Griessen, and M. W. McElfresh for key conversations which gave the initial incentive to this work, and L. Civale and J. R. Clem for further valuable discussions. In particular, Dr. Daeumling made to us the first suggestion to explain the radial dependence on the basis of the dominance of the dH_r/dz gradient.

[1]C. P. Bean, Phys. Rev. Lett. **8**, 250 (1962); Rev. Mod. Phys. **36**, 31 (1964).
[2]A. M. Campbell and J. E. Evetts, Adv. Phys. **21**, 199 (1972).
[3]F. M. Sauerzopf, H. P. Wiesinger, and H. W. Weber, Cryogenics **30**, 650 (1990).
[4]Y. Yeshurun, M. W. McElfresh, A. P. Malozemoff, J. Hagerhorst-Trewhella, J. Mannhart, F. Holtzberg, and G. V. Chandrashekhar, Phys. Rev. B **42**, 6322 (1990).
[5]D. J. Frankel, J. Appl. Phys. **50**, 5402 (1979).
[6]M. Daeumling and D. C. Larbalestier, Phys. Rev. B **40**, 9350 (1989).
[7]Y. B. Kim, C. F. Hempstead, and A. R. Strnad, Rev. Mod. Phys. **36**, 43 (1964).
[8]A. Sulpice, P. Lejay, R. Tournier, and J. Chaussy, Europhys. Lett. **7**, 365 (1988).
[9]H. Küpfer, I. Apfelstedt, R. Flükiger, C. Keller, R. Meier-Hirmer, B. Runtsch, A. Turowski, U. Wiech, and T. Wolf, Cryogenics **28**, 650 (1988).
[10]A. D. Hibbs and A. M. Campbell, IEEE Trans. Magn. **25**, 2142 (1989).
[11]M. Daeumling, J. Seuntjens, and D. C. Larbalestier, Appl. Phys. Lett. **52**, 590 (1988).
[12]M. Daeumling, J. M. Seuntjens, and D. C. Larbalestier, Nature **346**, 332 (1990).
[13]B. Oh, M. Naito, S. Arnason, P. Rosenthal, R. Barton, M. R. Beasley, T. H. Geballe, R. H. Hammond, and A. Kapitulnik, Appl. Phys. Lett. **51**, 852 (1987).
[14]T. R. McGuire, D. Dimos, R. H. Koch, R. B. Laibowitz, and J. Mannhart, IEEE Trans. Magn. **25**, 3218 (1989); and private communication.
[15]E. Shimizu and D. Ito, Phys. Rev. B **39**, 2921 (1989).
[16]W. R. Smythe, *Static and Dynamic Electricity* (McGraw-Hill, New York, 1950).
[17]G. Dahlquist and A. Bjorck, *Numerical Methods* (Prentice-Hall, Englewood Cliffs, New Jersey, 1974).
[18]W. Press, B. Flannery, S. Teukolsky, and W. Vetterling, *Numerical Recipes* (Cambridge University Press, New York, 1986).
[19]J. Stoer and R. Bulirsch, *Introduction to Numerical Analysis* (Springer, New York, 1980).